Research Article Open Access

Ioannis Mintourakis*

Adjusting altimetric sea surface height observations in coastal regions. Case study in the Greek Seas.

Abstract: When processing satellite altimetry data for Mean Sea Surface (MSS) modelling in coastal environments many problems arise. The degradation of the accuracy of the Sea Surface Height (SSH) observations close to the coastline and the usually irregular pattern and variability of the sea surface topography are the two dominant factors which have to be addressed. In the present paper, we study the statistical behavior of the SSH observations in relation to the range from the coastline for many satellite altimetry missions and we make an effort to minimize the effects of the ocean variability. Based on the above concepts we present a process strategy for the homogenization of multi satellite altimetry data that takes advantage of weighted SSH observations and applies high degree polynomials for the adjustment and their unification at a common epoch. At each step we present the contribution of each concept to MSS modelling and then we develop a MSS, a marine geoid model and a grid of gravity Free Air Anomalies (FAA) for the area under study. Finally, we evaluate the accuracy of the resulting models by comparisons to state of the art global models and other available data such as GPS/leveling points, marine GPS SSH's and marine gravity FAA's, in order to investigate any progress achieved by the presented strategy.

DOI 10.2478/jogs-2014-0012
Received April 10, 2014; accepted August 4, 2014.

1 Introduction

During the last decade a great effort has been in progress by the Geoscientific community in order to extend the use of satellite altimetry in coastal regions (Fernandes et al., 2002). This effort is driven by the need to resolve issues such as the unification of Local Vertical Datums (LVD), the precise marine geoid modelling near the shore for smooth transition from land to sea, and the assimilation of SSH observations in coastal ocean models. The main issues towards this progress is that the satellite altimetric data qualities over coastal seas decrease due to the weaknesses of the altimeters in the range tracking procedure close to the shoreline, and due to the complexity of the coastal tidal signals that are not modelled efficiently in the altimetric Geophysical Data Record (GDR) products. Regarding the range tracking issues there is a sustained related research on retracking algorithms (Sandwell and Smith, 2005; Andersen et al., 2010; Garcia et al. 2014), and also on the development of specialized projects and products such as the PISTACH products under the Coastalt project (Cipollini et al., 2008) and the ALTICORE project (Vignudelli et al., 2006), while there are additional tools such as X-track (Roblou et al., 2007).

As long as multi satellite altimetry missions are required for providing denser spatial resolution and extended temporal coverage, another issue that arises is the strategies followed for the processing and for the homogenization of multi satellite altimetry missions. The basic strategies are the stacking technique, that applies only to the almost collinear SSH observations that come from Exact Repeat Missions, the crossover adjustment (Tai and Fu, 1986; Rummel, 1993), and the conversion of the along track SSH/geoid slopes to deflections of the vertical (Sandwell, 1992), that applies only for the computation of the gravity anomalies. Each technique presents advantages and disadvantages but the results present a very good agreement between synchronous satellite altimetry derived, MSS and gravity FAA models over the open ocean. Although noticeable differences occur near the shoreline (Claessens, 2012) and they can be possibly attributed to the differences in the processing and in the homogenization strategies. The main concepts in processing SSH observations for MSS and marine geoid modelling are the elimination of the altimeter's noise from the observations, the removal of the satellite's orbital error and the minimization of the along track Sea Level Anomalies (SLA). As for the term homoge-

*Corresponding Author: Ioannis Mintourakis: School of Rural and Surveying Engineering, National Technical University of Athens, Zografou, 15780, Greece, E-mail: mintioan@survey.ntua.gr

nization strategies, this refers to the unification of SSH observations from multi satellite altimetry missions in a common epoch and in a common datum.

In the present paper we deal with the above concepts and produce a MSS, a marine geoid and a marine gravity FAA model. As a first step, we evaluate the statistical behavior of the SSH observations related to the range from the coast for various satellite altimetry missions. Based on this behavior we estimate an empirical model to describe the accuracy of the SSH observations in relation to the range from the coast for each satellite altimetry mission and a weight is assigned to each specific SSH observation. As a second step, we examine the contribution of high degree polynomials for the adjustment of subarcs with SSH observations in order to remove the orbital error and minimize the along track SLA's. At this point, we present the outcome of all the possible combinations for adjusting subarcs with weighted or without weighted SSH observations, and with or without the use of high degree polynomials. Based on the aforementioned outcomes we present an adjustment strategy, described as 'iterative subarc-levelling technique', for homogenizing the satellite altimetry SSH weighted observations with the use of high degree polynomials. For our case study, we estimate the regional MSS, marine geoid and gravity FAA's models for the seas around the Greek peninsula. The accuracy of the regional models is validated after comparisons to state of the art global models, which have used the same satellite altimetry datasets. Finally, all models (regional and global) are compared to many available independent datasets such as GPS/levelling points, marine GPS SSH's, and marine gravity FAA's in order to validate any progress achieved under the current project. Our test area is a demanding region for satellite altimetry due to the semi-enclosed Aegean Sea, the complex shorelines, the presence of hundreds of islands and the complexity of the regional short scale ocean circulation. The selected area is of (i) great geophysical interest, due to the subduction of the African plate under the South-Eastern European plate and due to the morphology of the seabed relief with plenty of short scale trenches, plateaus and basins, (ii) geodetic interest, due to the presence of numerous islands with independent LVD's, and (iii) oceanographic interest, due to the complex ocean circulation. The current project is motivated by the need to unify the independent LVD's present in Greece, and to develop the necessary models that will be used as frames for utilizing numerous datasets such as Digital Terrain & Bathymetry Models (DTBM), land & marine gravity, GPS/levelling benchmarks and tide gauge records for precise regional geoid modelling.

2 Investigations in processing the SSH observations

2.1 Statistical behavior of radar altimetry SSH near the coastline

It is well known that all radar satellite altimetry missions suffer from poor (noisy) performance near the coastal areas. This is mainly due to the weaknesses of the range tracking procedure being used onboard the processing unit of the altimeter (on-board tracker) to determine the exact time of the first reflection of the emitted pulse on the oceanic surface. Thus, a retracking procedure follows on the ground data processing centre where a fitting algorithm is applied to the waveform data in order to improve the on-board tracker range estimate. Although, both the on-board estimate and the retracking procedures suffer in coastal areas where there may be land contamination and other heterogeneities in the field of view sampled by the waveform. In the present study, we evaluate the statistical behavior of the SSH observations related to the range from the coast for the so-called Exact Repeat Missions (ERM) and the Geodetic Phases/Missions (GP/M) of several altimetry satellites. Specifically, we use ten years of the Jason-1 ERM SSH observations (Jan 2001-Dec 2011), 7 years of the Envisat ERM (Oct 2002-Aug 2009), the retracked (Lillibridge et al, 2006) Geosat Geodetic Mission (Mar 30 1985 – Sep 30 1986) and ERS-1 Geodetic Phase (Apr 10 1994 – Mar 21 1995), all the campaigns of the ICE-sat satellite carrying a laser-altimeter (Feb 20 2003-Oct 11 2009), and some of the first available cycles of the Cryosat-2 satellite (Jan 10 2012-Dec 31 2012). The SSH observations were computed and taken into account only when all the necessary geophysical corrections were present in the Geophysical Data Records (GDR), while there were no regional tidal or atmospheric models used.

Prior to any action, we have smoothed the along track SSH observations of every altimetric mission with the use of a 1.5 sec time domain full wavelength Gaussian filter. We came to adopt the 1.5 sec time domain full wavelength Gaussian filter after comparisons among various combinations of different filter types (Boxcar and Gaussian) and possible wavelengths. After visual inspection the adopted combination seemed to perform better in smoothing noisy SSH observations, while simultaneously resulting in a minimum loss of possible along track SSH short wavelength signals. In order to perform an analysis of the accuracy of each altimeter related to the range from the coast, the SSH observations should be referenced in a common epoch and Datum and should be free of orbit errors

and long wavelength ocean variability signals. For this reason every subarc of each satellite altimetry mission was fitted on an earlier version of the regional MSS. This earlier version of the MSS was determined after levelling the Geosat GM and the ERS-1 GP subarcs, with the use of a simple shift and tilt model, on a common mesh of Jason-1 and Envisat time averaged ERM profiles. As long as these SSH observations are considered as adjusted, any remaining SSH differences to the MSS correspond to two factors (i) the altimetric noise, and (ii) the short wavelength Sea Level Anomalies (SLA) present in the observations. Regarding the altimetric noise, it can be divided to two parts: one is a steady-white noise which corresponds to the altimeter precision under normal conditions, and the other part is an environment dependent noise. Close enough to the coast (eg in a range of 20 km) the second part is mostly affected by the 'land contamination' effect of the altimetric pulse. Regarding the SLA's, we assume, for the scope of studying the statistical behavior of the SSH differences near the coastline, that the remaining short wavelength SLA's have a smaller along track variation, and thus contribution, compared to the corresponding variations of the altimetric noise. Thus, we attribute the variations of the along track SSH differences close to the coastline entirely to the altimetric noise, and we relate them to the range from the coast in order to estimate the behavior of each altimeter. The above differences for each specific mission are studied in 2.5 km range sea sectors up to 20 km far from the coast and for each sector the standard deviation of the above differences is examined. At this point, we have to mention that the presence of long and medium wavelength errors in the MSS will result in biases and the resulting standard deviation of the SSH differences for a range sector will possibly represent mostly the MSS accuracy for that sector than the altimetric noise. For this reason the area under study is divided into local bins and the mean value of the SSH differences to the earlier MSS is computed for every local bin. Then this mean value is removed from the SSH differences of the corresponding bin, and we compute the standard deviation of all these 'reduced' SSH differences that are present in each range sector for all the area under study. Then the mean of the standard deviations from all the bins of a whole range sector is estimated and is representative of the altimetric noise for this range sector. In this way, the standard deviation of the SSH differences is estimated in each range sea sector for every altimeter.

Based on these results we fit a model of the form

$$y = f(x) \tag{1}$$

where, y is the standard deviation of the SSH differences, and x is the range from the coast (Fig. 1). As a function for $f(x)$ we pick a formula $a \cdot x^b$, where $b<0$ and x is the range from coast. For each satellite altimetry mission, the a and b parameters are estimated, and thus the empirical model that describes the altimetric noise related to the range from the coast.

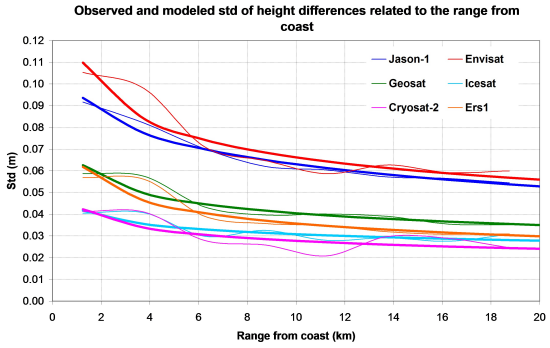

Fig. 1. The observed (hairline) standard deviations of the SSH differences and the modelled altimetric noise (heavy solid line) related to the range from the coast for each altimeter.

The results in Fig. 1 look reasonable as long as the implied accuracies at the range of 20 km distance from the coast (where in the almost absence of land contamination, the remaining noise corresponds to the previously mentioned white noise) for the Jason-1 and the Envisat are quite close to the standard deviations of Envisat/Envisat and Jason-1/Jason-1 SSH along track crossover differences (respectively 6 cm and 5.7 cm) presented in CLS.DOS/NT/12.021, 2011 yearly calibration/validation report. Regarding the Icesat altimeter the implied accuracy at the range of 20 km is close to the desired value of 3 cm standard deviation for clear water surfaces (Schutz and Zwally, 2008). Jason-1 and Envisat (both ERM's with classic pulse limited radar altimeter) present very similar behavior, while Geosat GM and ERS-1 GP, although equipped with classic pulse limited radar altimeter too, demonstrate better results due to the special retracked products used for the present study. Icesat and Cryosat-2 demonstrate almost identical results and seem to be almost immune to the presence of nearby coastlines. This is expected for the Icesat mission, since its Geoscience Laser Altimeter System (GLAS) has a very narrow footprint (~70 m in diameter) and is able to operate both over water and over land, but is surprisingly good for the Cryosat-2. For the Cryosat-2 satellite altimetry mission, we use the Low Resolution Mode (LRM) products. Although this means that it operates as a conventional pulse lim-

ited radar altimeter, Cryosat-2 in LRM mode is still sophisticated enough to adjust the pulse footprint from an area of approximately 2 km along-track for a completely calm sea, to 7 km or more, for a very rough sea (Stenseng and Andersen, 2012) and makes use of sophisticated retracking algorithms.

2.2 Removal of the orbital error & minimizing the SLA's

During the past, the main scope of an adjustment was the reduction of the orbital error since it was large enough. The problem of orbit modelling was an uncertainty in the initial state vector and this manifested itself as an error which was dominant once per revolution, thus a very long wavelength. For the reduction of the orbital error, and for regional studies, a sinusoidal or a simple shift and tilt model was considered adequate enough for describing the geometrical form of the error. But nowadays the once-per-rev error is very small, and the orbital ephemeris errors are more irregular and due to problems modelling the forces on the satellite, particularly as it enters into or emerges from the Earth's shadow. The orbital errors of all the satellite missions under study are small enough and well below the 10 cm level even for the Geosat GM which is the older of the missions. The retracked 20th anniversary product we use in the present study was reprocessed based on the GRACE gravity model GGM02C and has an estimated radial orbit error on the order of only 5 cm (Lillibridge et al, 2006). This magnitude of orbit errors is in most of the cases well below the sea surface variability present (or SLA's) in the observed SSH's along track of a subarc. The above points made us sceptical in using a linear or a simple sinusoidal model for removing the orbital error and for minimizing the sea surface variability. For this reason we decided to examine the outcome of adjusting subarcs with the use of a linear and of a high order polynomial, and by the use, or not, of the weights assigned to the SSH observations (based on the empirical models estimated in section 2.1). The test adjustment is made by 'levelling subarcs' on the former version of the regional MSS model presented earlier. As a high order polynomial we have used a Fourier (trigonometric) polynomial of 9 terms:

$$a_0 + \left(\sum_{k=1}^{4} (a_k \cos(kx) + b_k \sin(kx)) \right) \qquad (2)$$

The concept of the number of terms will be discussed later in the description of the adjustment strategy (section 3.1). At this point, we compute the difference between the adjusted SSH observations and the MSS model and we construct the grids of these differences by fitting a family of continuous curvature splines or applying the so-called tension gridding algorithm (Smith and Sandwell, 1990). Based on the visual inspection of these gridded height differences (Fig. 2) we notice the presence of linearly formed residuals that are significantly correlated with the ground tracks of the satellites (so-called as 'trackiness' effect).

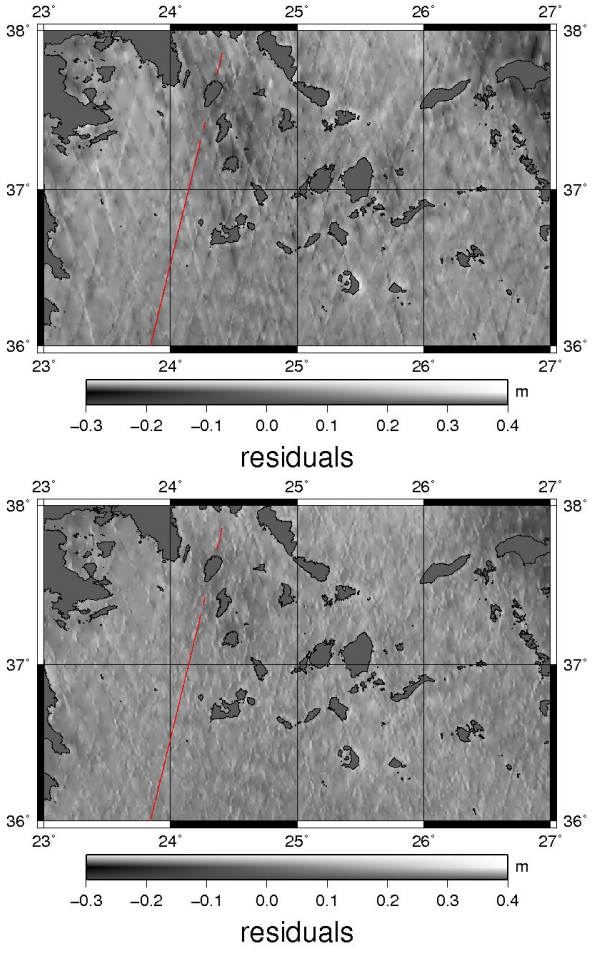

Fig. 2. The shaded relief of the gridded SSH residuals when the subarcs are adjusted (i) with the use of a linear model (top), (ii) with the use of a 9 terms Fourier polynomial (bottom). In the case of the adjustment with the use of a linear model it is evident that many cases of intense 'trackiness' effects are present. The red line is the footprint of an ERS-1 GP subarc along whose track SSH residuals are depicted in Fig. 3.

In order to investigate further the nature of these trackiness effects, we further inspect the plots of along-track SSH residuals and the corresponding linear trend and high degree polynomial adjustment models (Fig. 3). Based on these inspections, the presence of medium wavelength signals is evident. To what extend these differences can be attributed to SLA's or GDR errors is a scope of a

special study where these differences can be examined with other means (eg in conjunction with ocean circulation/SLA models). For the present we consider these differences as medium wavelength along track SLA signals that have to be minimized during the adjustment process. The main problem in MSS and geoid modelling is that the 'trackiness' effect is present on the generated surfaces and needs a filtering proportional to the size of the 'trackiness' in order to smooth it. Thus, it is evident that by using a linear trend model for the adjustment there will be a need to apply a more powerful filter, than in the case of a high degree model, for smoothing the 'trackiness' effect. So, we feel confident that the use of high degree polynomials for the adjustment process will prevent a great loss of the shorter wavelengths of the MSS signals due to extensive filtering.

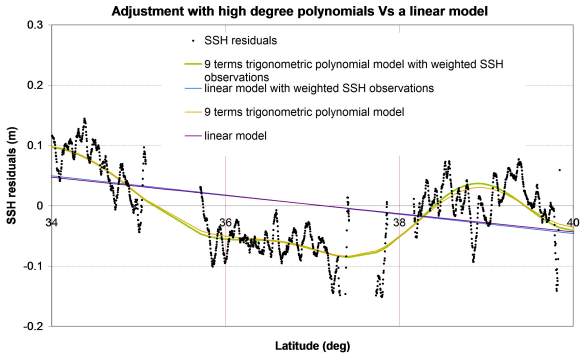

Fig. 3. The along track SSH residuals for an ERS-1 GP subarc intersecting the area in previous figure between the 36th and the 38th parallels that have generated a 'trackiness' effect along its track (Fig. 2). The differences between a linear and a 9 terns trigonometric polynomial reach up to a magnitude of 8 cm. Regarding the use of the weighted SSH observations during the adjustment process, we have to mention that their contribution is smaller than the resulting differences between the use of weighted and not weighted SSH observations which have a magnitude of up to 1.5 cm.

At this point we have to point out some facts (presented extensively in Sandwell, 1992; Olgiati et al, 1995) about the 'trackiness' effect and how crucial it is when estimating the free air gravity anomalies. As presented exactly, when satellite altimetry profile spacing decreases it becomes increasingly difficult to perform an adjustment on the original geoid height profiles without introducing large cross-track gradients on the modelled MSS. These cross-track gradients are the result of the 'trackiness' effect. It is known that the gradient of the geoids' surface is related to the vector of the gravity, and thus to the deflection of the vertical. As the deflection of the vertical is related to the vertical gravity gradient through the Laplace's equation, it is stated that 1 μrad of vertical deflection error translates to 0.98 mGal of gravity anomaly error. Assuming for the time, that the MSS presents the same gradients as the geoid, a 'trackiness' effect that introduces an error of 5 cm in a cross-track length of 5 km on the MSS, will result in a 10 μrad error. This means that across the miss-adjusted track, that generates the 'trackiness' effect to the MSS, an error of 9.8 mGal will be introduced.

2.3 Assigning weights to the SSH observations

Till now we have noticed that during the adjustment the use of high degree polynomials perform better than a linear model in reducing the combined effects of the orbital error and of the along track SLA's, and thus, in minimizing the 'trackiness' effect. Although after the adjustment the standard deviation of the remaining residual SSH's can vary up to a fraction of two for nearby parallel subarcs (with a separation of only a few kilometres) of the same altimetric mission. This difference in the standard deviations between the two neighbouring, parallel and almost identical subarcs can not be attributed to the pulse's land contamination effect, as long as the almost identical subarcs should have a similar amount of noise in their observations. After the adjustment, with the use of the high degree polynomials, the along track SLA signals are sufficiently smoothed but some residuals are still present. These remaining-unmodelled residuals can be associated to differences in the significant wave height form subarc to subarc and also to unmodelled tides and sea surface topography. For the present study we shall refer to these unmodelled residuals as remaining 'noise' after the adjustment of a subarc. This remaining 'noise' is equal to the standard deviation of the residuals of a subarc std_{arc} and is characteristic of the quality of the adjustment for each subarc.

When it comes to grid these SSH observations for MSS modelling, it is useful to have assigned weights depending on the noise of each SSH observation, as this will force the solution of the MSS to adopt better to the SSH observations with the reduced noise. This helps the gridding algorithm to be less sensitive to SSH observations of poor quality. Having available the model (Eq. 1) for describing the standard deviation, std_R, of the SSH observation related to the range from coast for each altimeter k, and the characteristic standard deviation of the remaining 'noise' in the adjusted SSH observations of a subarc j, std_{arc}, the

assigned weight w_i to each specific *SSH(i)* observation is:

$$w_i = \frac{1}{\sqrt{std_R^2 + std_{arc}^2}} = \frac{1}{\sqrt{(a \cdot x^{r(i)})_k^2 + std_{arc(j)}^2}} \quad (3)$$

where $(a \cdot x^{r(i)})_k$ is the k altimeters noise in its *SSH(i)* observation related to the range $r(i)$ of the point i from the coast.

3 Modelling the MSS and the marine geoid

The use of multi-mission altimetry data, and especially the combination of ERM with GP missions, offers a great advantage as it provides higher spatial resolution and greater coverage than the data from individual missions. While this fact is critical for the determination of the MSS and the marine geoid, some problems arise due to the different specifications and characteristics of each mission. When neglecting the observation noise, crossover differences correspond to the orbit errors, which are carrying the signature of errors in the Earth gravity field models, used for orbit determination and to the sea level variations between SSH observations at different times. Multi-mission crossover differences are minimized by multi-satellite orbit error determination, or by adjusting less accurate orbits using a more precise mission as a reference. This is done for missions that do not have very accurate orbit determination but also for removing biases and differences within the reference mission. Furthermore, each altimetric mission has different time coverage and refers to a different period of time, or epoch. Due to discrepancies at sea level between different epochs, all altimetric missions have to be unified at a common epoch. This is feasible by comparing and removing the SSH differences between each mission and a 'basic-reference' mission. In such a case, the ERM mission with the longer time coverage is preferred for being the reference mission as it provides the best estimate of the mean sea level across its observation points. The resulting MSS refers to the same period, or epoch, as the reference mission. Therefore, MSS-models that are based on different data periods are representative only for these periods.

3.1 Adjustment strategy

Crossover adjustment and stacking procedures are the most commonly used techniques for reducing along track differences in altimetric SSH observations, due to the radial orbit errors, to the sea level variability signal in the instantaneous SSH observations, and to a lesser extent, to the effects from errors in geophysical corrections applied to the data during pre-processing (Rummel, 1993; Knudsen, 1992). When applying a crossover adjustment for regional studies it is desirable to select a diamond shaped area bounded by two ascending and two descending satellite subarcs (Rummel, 1993). The presence of such a diamond shaped area is not always feasible for geographical regions with complex shorelines. Furthermore, during the adjustment of a subarc, in the event that the majority of crossover points are concentrated in one part of its subarc, the crossover adjustment process can possibly lead to biased parameters and consequently to a poorly set adjustment in the part with low density in crossover points. On the other hand, the stacking procedure does not pose similar problems as it operates co-linearly on the SSH observations of almost overlapping subarcs, which can be used to calculate time-averaged mean SSH profiles on their subarcs. In spite of this major advantage, the application of stacking techniques is only feasible for ERM missions which, however, do not offer dense coverage. For the present study, after taking into account all the aforementioned investigations in processing SSH observations, and the considerations regarding the complex geometry and the many different circulation patterns of the Aegean Sea, we decided to adopt a different strategy named as 'iterative subarc-levelling technique' for estimating a MSS from scratch.

During the 'iterative subarc-levelling technique' we take advantage of the Jason-1 and Envisat ERM's for building a reference frame, and the Geosat GM and ERS-1 GP for enhancing the signal resolution of the MSS (Fig. 4). The reference mission we use is the Jason-1 ERM as it provides both high precision in orbit determination and a long period of continuous observations. Moreover, both the earlier ERM of Topex/Poseidon, and the later ERM of Jason-2, have similar specifications and follow the same orbital tracks allowing the future expansion of the solutions with both earlier and later data and providing a reference frame of continuous SSH observations of more than 20 years.

Regarding the Jason-1 and Envisat ERM's we produce, separately for each mission, a 'network of time-averaged subarcs'. Each of these so-determined mean altimetric profiles corresponds to a set of averaged sea surface heights, along the repeated (nearly co-linear) satellite subarcs of each satellite. The mean altimetric profiles are computed assuming all SSH's observations have equal weights as we believe that applying weights to the observations of the ERM missions has nothing to offer in this averaging process. In turn, the network they form is

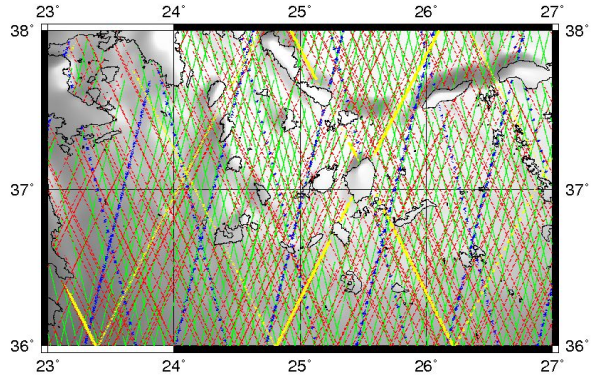

Fig. 4. The distribution of satellite altimetry observations used in the present paper for the area of the central Aegean Sea. The ERM missions Jason-1 (yellow colour) and Envisat (blue colour) provided the reference frame, while the Geosat GM (red colour) and the ERS-1 GP (green colour) enhance the spatial resolution.

representative of the regional mean sea surface for the period of time on which the SSH observations were collected. This averaging process is essentially used to get rid off (i) most of the effects from variable phenomena (such as seasonal variability, semi-annual, inter-annual) whose period is shorter than the period of the available measurements, and (ii) from orbit errors. Since Jason-1 is set as the reference mission, the network of mean altimetric profiles from Envisat is brought to the level of the corresponding Jason-1 network by simply removing, for each Envisat time-averaged subarc, the mean of its SSH differences at the crossover points formed with the corresponding Jason-1 time-averaged profiles obtained from the previous step. In this way, the data sets of the two missions are homogenized, creating a common mesh of compatible time-averaged and mutually levelled profiles, which provides a denser coverage of the area of interest than using only one of the two ERMs. In the sequel, we shall refer to these time-averaged and mutually levelled Jason-1 and Envisat profiles, simply as the (Jason-1/Envisat) 'Mean Homogenized Altimetric Profiles' or MHAPs for short. Having this common mesh of MHAPs as a reference frame, all other SSH profiles from the Geosat GM and ERS-1 GM missions were similarly reduced, subarc-by- subarc, to the common Jason-1/Envisat mesh by removing, in a point-by-point fashion within each profile, the mean of the SSH differences observed at the intersections of each profile with the previously determined Jason-1/Envisat MHAPs reference frame. This process essentially resulted in a computationally quick homogenization of all the available multi-satellite SSH datasets, without the need to perform a grand multi-satellite crossover adjustment with more complex patterns of crossover combinations between ascending and descending subarcs and between different satellite pairs.

In a third step, we use the entire dataset of the so-mutually levelled SSH profiles from all missions, for creating an intermediate MSS by using the tension gridding technique (Smith and Wessel, 1990). Then we apply a smoothing Gaussian filter using the grdfilter program of the Generic Mapping Tools (GMT) suite (Wessel & Smith, 2012), on this intermediate MSS in order to remove any residual altimetric noise, medium to short wavelength ocean variability, and miss-adjustment effects. Regarding the applied filter, we have made some trials with different wavelengths and visualised their gradient effects. After visual inspection of their gradient effects, and taking into account the spatial distribution of the altimetric SSH observations (bearing in mind that the average distance between parallel MHAPs does not exceed 60 km), we consider that a 120 km full wavelength Gaussian filter is adequate enough. This process results in a smooth reference mean sea surface (MSSref) for the area of interest, which can be considered as a regional MSS of low resolution, that can be used in a loop scheme for the adjustment of the SSH observations. For each single subarc j the difference:

$$\Delta_{t,j} = SSH_{t,j} - MSS_{ref} \tag{4}$$

is computed, where $SSH_{t,j}$, is the instantaneous SSH point value measured by the altimeter at time t during the j pass of the satellite subarc, and MSS_{ref} is the interpolated height value of the reference MSS at the given point. At this step, having available the statistics of the mean and of the standard deviation values of the $\Delta_{t,j}$ differences, we are able to reject any spurious along subarc j, $SSH_{t,j}$ observations that fail to pass a test criterion of

$$mean_j - a \cdot std_j \le \Delta_{t,j} \le mean_j + a \cdot std_j \tag{5}$$

or even reject a specific subarc j if the standard deviation value of the $\Delta_{t,j}$ differences is greater than a maximum acceptable value. The computed differences $\Delta_{t,j}$ for each subarc can be approximated, by a regression model

$$y = f(x) + e \tag{6}$$

in a weighted (as long as the weights for each observation are available) least squares sense, where $f(x)$ may be chosen as polynomial or Fourier (trigonometric), with the use of the trend1d program of the GMT suite (Huber, 1964; Menke, 1989; Wessel & Smith, 2012). The adjusted SSH's then form a new reference MSS_{ref}, of higher resolution to the previous one (by applying a shorter wavelength cut of filter), and the new differences $\Delta_{t,j}$ for each subarc can be approximated by a regression model of higher order. During this loop scheme the resolution of the reference MSS_{ref}

is raising, and so the order of the regression model used for the adjustment until two consecutive solutions of the MSS_{ref} are practically the same (e.g. the standard deviation of their difference drops bellow a desired limit).

The advantages of the above described adjustment strategy are numerous as it:

- Permits the rejections of along-track spurious observations before the fitting of the subarc.
- Permits the rejection of a whole subarc (e.g. if the standard deviation of its $\Delta_{t,j}$ is above a critical value).
- Can use the standard deviations of the SSH observations related to the range from coast, std_R, as weights during the adjustment process.
- Can estimate the standard deviation of the remaining noise std_{arc} in the SSH observations after the adjustment of a subarc.
- Applies the fitting model based on the computed differences $\Delta_{t,j}$, for all the observations of the subarc and not only for the differences at the crossover points (as in a common crossover adjustment). In this way it takes advantage of a greater number of dense observations.
- Can include an additional model in the regression step having a physical meaning. For example, a model that fits the position of the sun or the moon in order to investigate if the local tide models can be improved.
- Can be used in a loop scheme where the adjusted SSHs form a new MSS_{ref} and the adjustment is run again until a selected convergence criterion is accomplished between two consecutive solutions.
- Has a small demand in computational power as it runs subarc by subarc and does not form a huge array of observations as in a crossover adjustment algorithm.

We have to state a point that someone should pay attention when applying the loop scheme during the presented methodology. As long as the length of the subarcs is not the same, we should consider that applying a high degree regression model to a short subarc would lead to aliasing. This is because the high degree regression model will force the along track SSH observations of a short subarc to adopt the MSS_{ref} values and consequently this would lead to a loss of true along track signals. Thus, the shorter wavelength implied by the number of model terms should be always sufficiently longer than the shorter wavelength present in the MSS_{ref}. In order to avoid such aliasing effects, we need to know which wavelengths are fitted by the model and which is the shortest wavelength we need to fit during a loop. For this reason we believe that the use of the Fourier model is more appropriate than the simple polynomial model and we suggest two options for avoiding such aliasing. The first is the use of a number of model terms proportional to the length of the subarc, and thus proportional to the shorter wavelength that we need to fit. The second option is iteratively increase the number of model terms, starting at one, until a maximum accepted number of terms is reached or the reduction in variance of the model is not significant at a selected confidence level. A third option is the combined use of both options where the maximum accepted number of model terms in the second option is set proportional to the length of the subarc.

3.2 The regional MSS, marine geoid and gravity FAA models

In our case study, we applied the 1st option and after following the above described 'iterative subarc-levelling technique' we estimated the final MSS after 4 loops. During the last loop the regression model used for the adjustment is a trigonometric polynomial of 7, 9 and 13 terms, for the short (<300 km), medium (300 km up to 600 km) and long (>600 km) subarcs respectively (Table 1).

Table 1. The full wavelength of the smoothing Gaussian filter applied in the MSSref, and the number of terms of the trigonometric polynomial used during the adjustment of the medium length subarcs used in each loop.

loop	full wavelength (km)	number of terms
1	120	3
2	60	5
3	40	7
4	20	9

At this point, the adjusted and weighted SSH observations, as described in section 2.3, can be used in a Least Squares Collocation (LSC) with weights gridding algorithm and the final National Technical University of Athens MSS Version 1 (NTUAMSSv1) is computed for the area under study (Fig. 5, top). In an alternative option, we neglected the weights of the observations and used the adjustable tension continuous curvature surface gridding algorithm of the GMT suite (Smith and Wessel, 1990) and then applied a 14 km full wavelength smoothing Gaussian filter for building the final MSS. We have to notice that this option performs much faster than the LSC without noticeable differences between the two surfaces. Either the LSC with weights, or the GMT suite surface algorithm processes are done in a RCR fashion, in order to perform the gridding on a smooth field with small range of height variations. Thus, during the remove and the restore steps we subtract and

add back the contribution of the EGM2008 (Pavlis et al., 2008) model expanded up to 2160 degree and order, realized in the mean tide system, and the contribution of the Synthetic Mean Dynamic Topography RIO07 (Rio et. al., 2007) model for the Mediterranean Sea.

If during the restore step the SMDT RIO07 model is not restored back, the resulting surface is the geoid computed in an oceanographic approach. In this way we create the NTUA Marine Geoid Version 1 (NTUAMGv1) model and the corresponding marine gravity NTUA FAA Version 1 (NTUAFAAv1) model. Regarding the FAA model it is also computed in a RCR fashion where the contribution of a geopotential model to the geoid heights is removed from the NTUAMGv1 model, and the inverse Stokes integral with the use of Fast Fourier Transform (FFT) is applied on the residual geoid grid for estimating the residual gravity anomalies. The residual gravity anomalies are then low passed with a 14 km full wavelength Gaussian filter. Finally, the contribution of the geopotential model to the free air gravity anomalies is restored to the residual gravity anomalies grid and the final NTUAFAAv1 model is estimated (Fig. 5, bottom). As a reference geopotential model we use once again the EGM2008 model (Pavlis, 2008) at full degree and order.

As a remark, we have to notice about the final Gaussian filter type and the 14 km full wavelength applied that in the present case they were decided after comparing to in-situ data the resulting MSS, geoid and free air gravity anomalies models of many different combinations of filter types (Gaussian and Boxcar) and wavelengths (from 9 km up to 20 km full wavelength). During this process, we took into consideration (i) the 1.5 seconds along-track Gaussian filter, discussed in section 2.1, and (ii) the cross track spacing (4 – 8 km) of the altimetric observations available from Geosat GM and ERS-1 GP. These two factors define the shortest possible wavelength of the applied filter as it does not make any sense to apply a filter of full wavelength shorter than (i) that applied during the along track filtering, or (ii) the double of the average cross track spacing.

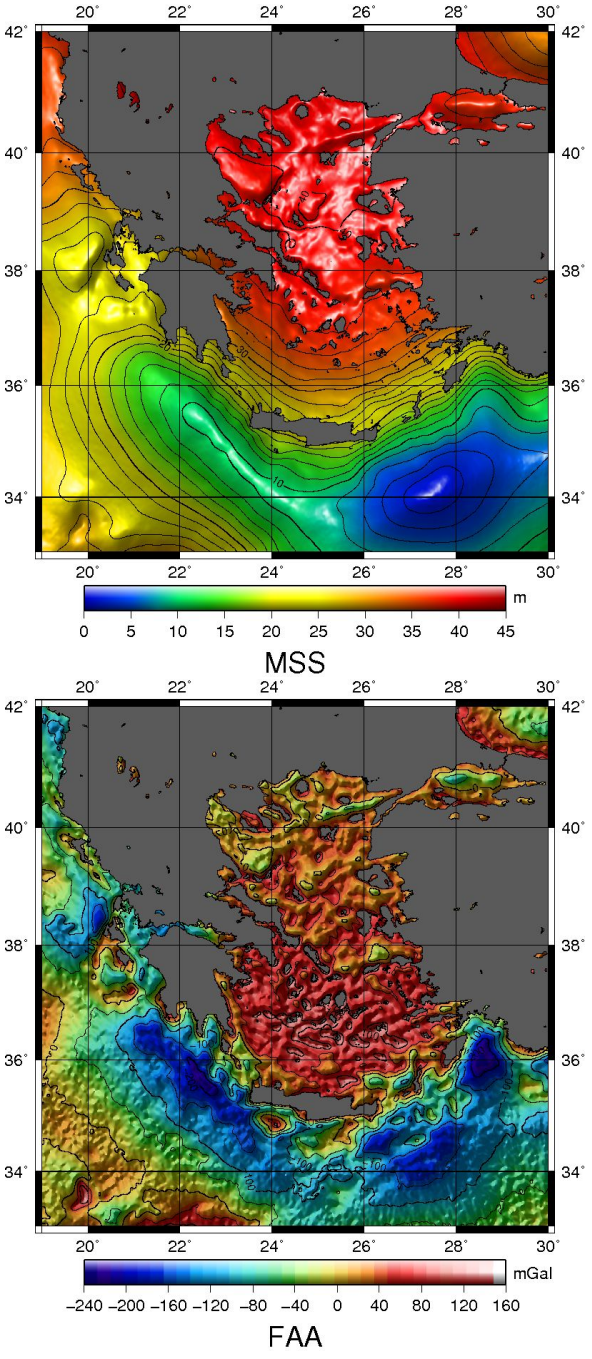

Fig. 5. Top, the NTUAMSSv1 model (contour interval 2 m). Bottom, the marine gravity NTUAFAAv1 model (contour interval 50 mGal).

4 Comparisons

Till now we have presented the adjustment of weighted SSH observations with the use of high degree polynomials implemented in the 'iterative subarc-levelling technique' homogenizing strategy. In order to validate any possible progress in marine geoid modelling, we compare the regional models to global models that have used the same satellite altimetry missions. Thus, we make comparisons to the state of the art Sandwell and Smith Satellite global Free Air Gravity V20 model, from now on denoted as SSv20 (Sandwell and Smith, 2009), the Danish Technical University 2010 global gravity field and global MSS model, from now on denoted as DTU10grav and DTU10MSS (Andersen, 2010), and the EGM2008. Finally, we present many intercomparisons of all these models with regional data. Since

the DTU10MSS, DTU10grav and SSv20 use as basic satellite altimetry missions for recovering the shorter signals of the marine gravity field and the shorter wavelengths of the MSS, the Geosat GM and the ERS-1 GP retracked products, we decided to incorporate only the aforementioned products in our regional models for the purpose of the following comparisons. We took this decision as we needed to asses the results of the processing strategy and not to present the contribution of the later satellite altimetry missions. For this reason, the updated Version 2 models will follow soon and will include the apparently superior Cryosat-2 and ICEsat and the Jason-1 GP satellite altimetry data.

From a visual inspection we have noticed that all models agree for the open ocean for a range of 50 km from the coastline, and that all the major differences are concentrated near the coast (Table 2 and Table 3). Analytically, based on the variations between the open ocean and the coastal regions, we notice that all the extreme height and gravity anomalies differences are concentrated close to the coast.

Table 2. The NTUAMSSv1 height differences to the DTU10MSS and the NTUAMGv1 height differences to the EGM2008 for the open ocean and for the coastal regions. There are noticeable variations between the entire and the coastal region, while it is clear that all the extreme differences occur in the coastal regions.

(m)	open ocean		coastal regions	
	DTU	EGM	DTU	EGM
mean	0.065	0.108	0.076	0.072
rms	0.022	0.060	0.082	0.102
min	−0.046	−0.082	−0.763	−0.456
max	0.221	0.407	1.337	0.632
range	0.267	0.489	2.100	1.088

As we find the above described disagreements close to the coast quite interesting, we make similar comparisons with in-situ data in order to ascertain if the disagreements are caused by errors in our models. The in-situ data (Fig. 6) are marine gravity FAA's available for download from the SISMER (Systèmes d'Informations Scientifiques pour la Mer) database, 'geoid' heights obtained by GPS observations of WGS-84 ellipsoidal heights on survey monuments with orthometric heights in local datums (so on mentioned as GPS/levelling benchmarks), and an ultra-regional marine GPS derived MSS model (Mintourakis & Delikaraoglou, 2010).

We cross-validate all models with this regional data, using the GMT *grdtrack* bicubic interpolation algorithm (Wessel and Smith, 2012), and we present the results in

Table 3. The NTUAFAAv1 gravity anomalies differences to the DTU10grav, to the EGM2008 and to the SSv20 for the open ocean and for the coastal regions. Regarding the variations between the entire and the coastal region, all the extreme differences occur in the coastal regions as in the case of the MSS and geoid height differences.

(mGal)	open ocean		
	DTU	EGM	SS
mean	0.291	0.273	1.719
rms	2.173	2.257	2.599
min	−12.304	−13.520	−13.900
max	12.263	12.731	16.279
range	24.567	26.251	30.179
(mGal)	coastal regions		
	DTU	EGM	SS
mean	−0.578	−0.527	0.234
rms	3.850	4.166	6.731
min	−23.908	−26.325	−87.606
max	26.947	27.671	88.285
range	50.855	53.996	175.891

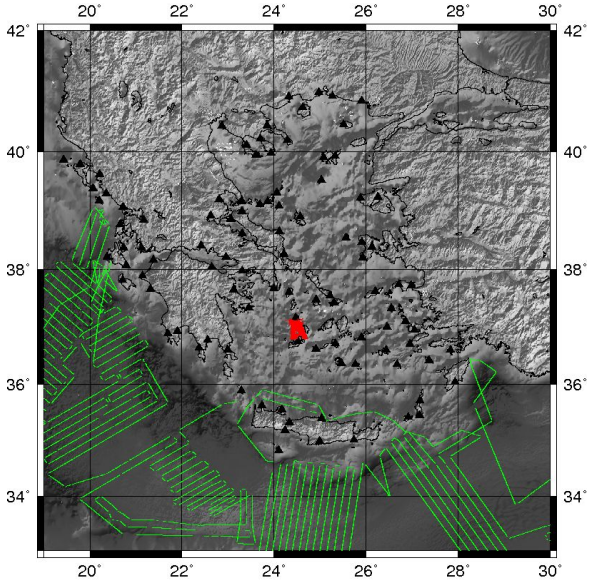

Fig. 6. The in-situ marine gravity (green lines), marine GPS (red area) and GPS/levelling (black triangles) data sets.

Tables 4, 5 and 6. Regarding the comparisons with the GPS/levelling benchmarks (Table 4) we have to notice that, although they are located very close to the coast, extrapolation errors occur on the surfaces generated by the gridding algorithms applied in each model, due to lack of satellite altimetry observations on land. We decided to make such comparisons as we do not have any GPS/levelling observations located on the coast (e.g. GPS observations on tidal stations) and this is the only possible height comparison we can present very close to the coast. Furthermore, as

there are many LVDs in the Greek region, the GPS/levelling dataset have biases and thus it is risky to make any conclusions. Although we have to notice that the results in table 4 present a slight improvement of the regional models to the EGM2008 model close to the coastline. Analytically, there is an improvement in the order of 2 cm regarding the rms value and around 19 cm in the range of extreme differences. Another comparison we present is similar to the one used for the evaluation of the EGM2008 in the Greek area (Kotsakis et al, 2009). In this case we computed the differences

$$\Delta = \Delta N_{ij}^{GPS} - \Delta N_{ij}^{\mathrm{mod}\ el} \tag{7}$$

for all the 4950 possible baselines formed within the network of the 100 GPS/levelling benchmarks and we estimated the rms of these differences as a function of the baseline length for all models (Fig. 7). The availability of a large GPS/levelling dataset, as the one in the evaluation of the EGM2008, would permit us to make extended comparisons of the regional and the global models and draw some interesting conclusions (e.g. study the behaviour of the many independent LVDs). Till then, the only conclusion we can draw is that the regional models present a small improvement compared to the global models.

Table 4. The height differences of all models compared to a set of 100 GPS/levelling benchmarks located up to 5 km from the coastline.

(m)	NTUAMSS	NTUAMG	DTU	EGM
mean	0.225	0.232	0.035	0.150
rms	0.147	0.152	0.253	0.170
min	−0.220	−0.202	−1.308	−0.471
max	0.690	0.645	0.802	0.601
range	0.910	0.847	2.110	1.072

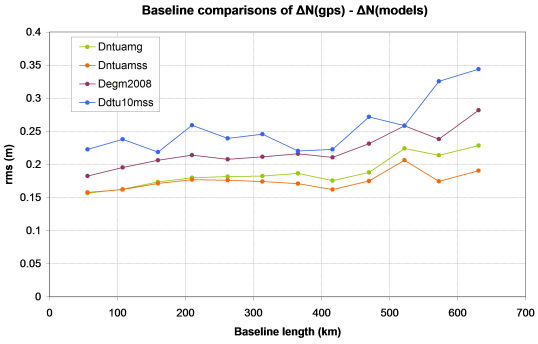

Fig. 7. Standard deviation of the differences $\Delta N_{ij}^{GPS} - \Delta N_{ij}^{\mathrm{mod}\ el}$ in the network of the 100 GPS/levelling benchmarks as a function of the baseline length.

In the past we have created an ultra regional MSS model derived from marine GPS SSH observations collected in the Central Cyclades Islands (Mintourakis and Delikaraoglou, 2010). This model has high resolution and internal accuracy, but lacks external accuracy as there were issues with the calibration of the absolute antenna height from the vessels' waterline, and thus, it was referenced to the KSMSS04 model (Knudsen et al., 2005) which is the predecessor of the DTU10MSS model. As this ultra regional MSS model has very high resolution and extends very close to the coast, we use it for further comparisons. Based on the results (Table 5) we find that the newly compiled regional models are accurate enough as they present the best agreement in terms of the rms value to the ultra regional MSS model.

Table 5. The height differences of all models compared to ultra regional MSS derived from marine GPS SSH's.

(m)	NTUAMSS	NTUAMG	DTU	EGM
mean	0.140	0.141	0.018	0.054
rms	0.031	0.028	0.039	0.054
min	0.022	0.018	−0.069	−0.062
max	0.237	0.232	0.123	0.195
range	0.216	0.213	0.192	0.256

As a final test we compare all the models to marine gravity data. Regarding the power spectrum and the coherency of all the satellite altimetry derived gravity models to the marine gravity observations (Fig. 8) the SSv20 and the NTUA models present a similar power spectrum in the shorter wavelengths band (10 – 30 km). In the same band, the SSv20 presents the best coherency to the marine gravity observations, followed by the NTUA model. The DTU model presents practically the same spectral characteristics to the EGM2008 model with an obvious drop of its signal power, and a steep loss of the presented coherency below the 25 km wavelengths.

The above highlights the advantages of the technique applied for computing the SSv20 gravity field as it allows the conversion of the along track SSH/geoid slopes to deflections of the vertical without the need to obtain first the geoid surface, and thus, without the need to apply extensive filtering for smoothing any miss-adjustments of the SSH observations. This problem is more obvious in the DTU power spectrum and to its coherency diagram. On the other hand, although the NTUA model was similar to the DTU model geoid to gravity conversion technique; it presents a power spectrum very close to the SSv20 model. Furthermore, the coherency diagram presents below the

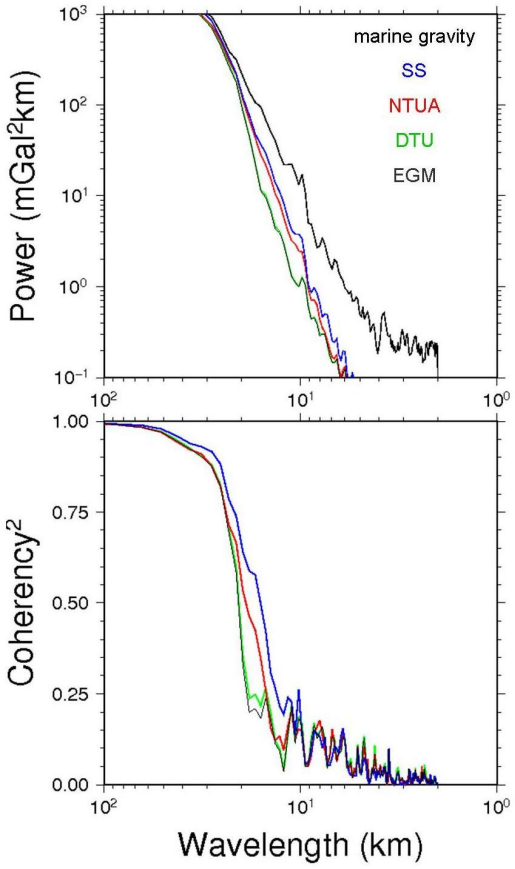

Fig. 8. The power spectrum and the coherency of the satellite altimetry derived gravity models related to the marine gravity observations.

30 km wavelengths a loss of the NTUA model coherency to the marine gravity observations smoother than that of the DTU model. The above comparisons between the NTUA and the DTU models point out that the presented adjustment strategy, with the use of high degree trigonometric polynomials and weighted SSH observations, is yielding to an improvement in the shorter gravity signals and thus the shorter wavelengths of the geoid that they have been derived from.

Next we examine the statistical values of the comparisons between the satellite altimetry derived gravity models and the marine gravity data. The results present almost identical statistical values with a slightly better rms value for the SSv20 model and a smaller range of extreme differences for the NTUA model (Table 6).

As presented in Table 3, the biggest differences between all models exist in the coastal regions. Thus, as we need to investigate the discrepancies of the regional model to the global models close to the coastlines, we split the comparisons, presented in Table 6, in 5 range sea sectors,

Table 6. The differences of the gravity anomalies models compared to marine gravity cruises.

(mGal)	NTUA	EGM	DTU	SSv20
mean	0.532	0.217	0.279	−1.310
rms	3.156	3.236	3.134	2.961
min	−19.324	−24.012	−23.197	−22.933
max	15.227	16.850	17.080	15.280
range	34.552	40.862	40.277	38.213

each of 10 km width, extending from the coastline up to 50 km from it (Table 7).

Based on the results presented in Table 7, both the NTUAFAAv1 and the SSv20, if we exclude the 0 – 10 km sector where SSv20 presents its worst statistical values, models present a best performance and a shortest variation of their statistical values compared to the corresponding performance and variations of the DTU10grav and the EGM2008 models. When we examine the comparisons in the 0 – 10 km coastal sector the NTUAFAAv1 performs better above all models as it presents the best rms and the shortest range of differences. Based on these comparisons the new regional model presents a good performance in the coastal regions and the smoothest transition from the open ocean up to the coastline above all models.

5 Conclusions

In the present paper we presented some of the basic concepts someone faces when processing satellite altimetry data in coastal regions. Based on the analysis of these concepts we investigated the contribution of adjusting subarcs, of weighted SSH observations with the use of high degree polynomials, and presented the corresponding strategy for computing the MSS. The new regional MSS, marine geoid and gravity anomalies models were compared with state of the art global models that have used the same satellite altimetry datasets. After the first findings, all models were cross validated extensively with the use of independent terrestrial and marine data. Based on these validations we found that our process strategy results to an improvement in the MSS and marine geoid modelling. Regarding the contribution of the presented strategy in the marine gravity field modelling, it offers a slight improvement very close to the coastline. The spectral characteristics of the regional NTUAFAAv1 model are slightly inferior to the SSv20 model but better than the DTU10grav that follows the same approach for computing the gravity field through the applications of the inverse Stokes integral on

Table 7. Statistics of differences with marine gravity at various distances from the coast (from top to bottom: mean, standard deviation, range of differences).

model	0-10km	10-20km	20-30km	30-40km	40-50km	>50km
#points	507	1502	1878	1572	1972	33380
			mean (mGal)			
NTUA	0.403	1.208	0.449	0.490	0.341	0.522
EGM	−0.491	1.472	0.197	−0.040	−0.234	0.211
DTU	0.413	1.376	0.666	0.283	0.044	0.221
SSv20	−2.167	−1.560	−1.499	−1.601	−1.832	−1.232
			rms (mGal)			
NTUA	6.295	5.365	5.215	3.873	3.804	2.685
EGM	7.318	6.265	5.450	4.375	4.458	2.539
DTU	6.823	5.940	5.427	4.310	4.415	2.453
SSv20	9.011	5.591	4.878	4.420	4.221	2.188
			range of differences (mGal)			
NTUA	28.575	32.297	33.024	28.334	32.684	32.475
EGM	40.596	35.248	38.949	26.136	38.276	32.704
DTU	39.379	34.803	38.319	25.588	37.180	31.508
SSv20	38.213	32.489	30.080	24.171	29.916	24.017

the geoid surface. A task for the future is the computation of the gravity FAA's model following the conversion of along track SSH/geoid slopes (coming from the adjusted subarcs) to gravity anomalies in order to examine any possible improvement in gravity field modelling. All validation results show that the strategy we have followed resulted in models fine-tuned in coastal regions. Thus, we believe that the present research can contribute positively to satellite altimetry coastal applications such as the unification of LVDs and the marine geoid/gravity field modelling.

Acknowledgement: The author wishes to thank W.H.F. Smith and D.Delikaraoglou for their valuable suggestions and comments, and J.Lillibridge for providing great help regarding the Geosat GM 20th Anniversary Product.

References

Andersen O.B., Knudsen P. and Philippa A.M.B., 2010, The DNSC08GRA global marine gravity field from double retracked satellite altimetry, Journal of Geodesy, vol.84, pp 191-199.

Andersen O.B., 2010, The DTU10 Gravity field and Mean sea surface, presented in "Second international symposium of the gravity field of the Earth (IGFS2)" Symposium, Fairbanks, Alaska.

Cipollini P., Gómez-Enri J., Gommenginger C., Martin-Puig C., Vignudelli S., Woodworth P. and Benveniste J., 2008, Developing radar altimetry in the oceanic coastal zone: the COASTALT project, presented at EGU General Assembly 2008, Vienna, Austria, 13-18 April, 2008.

Claessens S.J., 2012, Evaluation of Gravity and Altimetry Data in Australian Coastal Regions, Geodesy for Planet Earth, International Association of Geodesy Symposia, vol. 136, pp 435-442.

Fernandes M. J., Bastos L., Antunes, M., 2002, Coastal Satellite Altimetry Methods for Data Recovery and Validation. In I.Tziavos (ed.), 3rd Meeting of the International Gravity & Geoid Commission GG2002, Editions ZITI, pp 302-307.

Garcia E.S., Sandwell D.T. and Smith W.H.F., 2014, Retracking CryoSat-2, Envisat and Jason-1 radar altimetry waveforms for improved gravity field recovery, Geophysical Journal International, vol. 196, issue n.3, pp 1402-1422.

Huber P.J., 1964, Robust Estimation of a Location Parameter, The Annals of Mathematical Statistics, vol. 35, no. 1, pp 73-101.

Kotsakis C., Katsambalos K., and Gianniou M., 2009, Evaluation of EGM08 based on GPS and orthometric heights over the Hellenic mainland, Newton's Bulletin - External Quality Evaluation Reports of EGM08, issue n.4, pp 144-163.

Knudsen, P., 1992, Altimetry for Geodesy and Oceanography. In Geodesy and Geophysics, pp 87-129, Finnish Geodetic Institute.

Knudsen P., Vest A.L. and Andersen O.B., 2005, Evaluating mean dynamic topography models within the GOCINA project. ESA SP–572.

Lillibridge J., Smith W.F.H., Sandwell D., Scharroo R., Lemoine F.G. and Zelensky N.P., 2006, 20 Years of Improvements to GEOSAT Altimetry, presented in "15 Years of Progress in Radar Altimetry" Symposium, Venice, Italy.

Menke, W., 1989, Geophysical Data Analysis: Discrete Inverse Theory, Revised Edition, Academic Press, San Diego.

Mintourakis I., and Delikaraoglou D., 2010, Comparison between GPS sea surface heights, MSS models and satellite altimetry data in the Aegean Sea. Implications for local geoid improvement. In S.Mertikas (ed.), Gravity Geoid and Earth Observation GGEO2008, International Association of Geodesy Symposia, vol.135, pp 67-73.

Olgiati A., Balmino G., Sarrailh M. and Green C.M. , 1995, Gravity anomalies from satellite altimetry comparison between computation via geoid heights and via deflections of the vertical, Bulletin Geodesique, vol.69, pp 252-260.

Pavlis N., et al, 2008, An Earth Gravitational Model to Degree 2160: EGM2008, Presentation given at the 2008 European Geosciences Union General Assembly held in Vienna, Austria.

Rio M.H., Poulain P.M., et al., 2007, A Mean Dynamic Topography of the Mediterranean Sea computed from altimetric data, in-situ measurements and a general circulation model, Journal of Marine Systems vol.65: pp 484-508.

Roblou L., Lyard F., Le Henaff M. and Maraldi C., 2007, X-TRACK, a new processing tool for altimetry in coastal oceans, proceedings 'Envisat Symposium 2007', 23-27 April 2007, Montreux, Switzerland, ESA SP-636.

Rummel R. , 1993, Principle of Satellite Altimetry and elimination of Radial Orbit Errors, Lecture Notes in Earth Sciences No 50, Springer Verlag, pp 190-241.

Sandwell D.T., 1992, Antarctic marine gravity field from high-density satellite altimetry, Geophysical Journal International, vol.109, pp 437-448.

Sandwell D.T. and Smith W.H.F., 2005, Retracking ERS-1 altimeter waveforms for optimal gravity field recovery, Geophysical Journal International, vol.163, pp 79-89.

Sandwell D.T. and Smith W.H.F., 2009, Global marine gravity from retracked Geosat and ERS-1 altimetry: Ridge segmentation versus spreading rate, Journal of Geophysical Research, vol.114, issue B01411.

Smith W.H.F. and Wessel P., 1990, Gridding with continuous curvature splines in tension, Geophysics, vol.55, no.3, pp 293-305.

Schutz, B.E. and Zwally H.J., 2008, Overview of the Science Results from ICEsat, Proceedings of the 16th International Workshop on Laser Ranging, Poznan.

Stenseng, L. and Andersen O.B., 2012, Preliminary gravity recovery from CryoSat-2 data in the Baffin Bay, Advances in Space Research, vol.50, issue.8, pp 1158-1163.

Tai C.K., and Fu L.L., 1986, On crossover adjustment in satellite altimetry and its oceanographic implications, Journal of Geophysical Research, vol.91, issue C2, pp 2549-2554.

Vignudelli S., Cipollini P., Snaith H.M., Venuti F., Lyard F., Roblou L., Kostianoy A., Lebedev S. and Mamedov R., 2006, ALTICORE: an Initiative for Coastal Altimetry, International Workshop on coast and land applications of satellite altimetry, Beijing, China, July 21-22, 2006, pp 51-52.

Wessel P. and Smith W.H.F., 2012, The Generic Mapping Tools (GMT) version 4.5.8 Technical Reference & Cookbook, SOEST/NOAA.